Fault Detection of the Cylindrical Plunge Grinding Process by Using the Parameters of AE Signals

Jae-Seob Kwak*, Ji-Bok Song
School of Mechanical Engineering, Pusan National University

The focus of this study is the development of a credible fault detection system of the cylindrical plunge grinding process. The acoustic emission (AE) signals generated during machining were analyzed to determine the relationship between grinding-related faults and characteristics of changes in signals. Furthermore, a neural network, which has excellent ability in pattern classification, was applied to the diagnosis system. The neural network was optimized with a momentum coefficient, a learning rate, and a structure of the hidden layer in the iterative learning process. The success rates of fault detection were verified.

Key Words : Fault Detection, Acoustic Emission Signal, Neural Network

1. Introduction

In recent years, the grinding operation has been used in precision machining when surface roughness and/or geometric tolerances cannot be met by traditional cutting operations. With the necessity of near net-shape technology for precision components, the demand for the improvement of grinding performance will increase. However, there are unique characteristics in the grinding process. For example, as opposed to a turning tool, grinding wheels contain many grains that are randomly spaced and occupied within the periphery of the wheel. For this reason, a mathematical approach to studying the grinding process includes many functional parameters that cannot certify to their quantitative relations (Lindsay and Hahn, 1971; Kim et al., 1994).

A grinding burn, which is one of the faults occur to a ground surface, is related to the thickness of the oxide layer, which in turn is affected by the maximum temperature at the cutting zone (Kawamura and Mitsuhasi, 1981). The generated burn deteriorates the surface performance of a product. Another fault is chatter vibration, which is a relative motion between the grinding wheel and the workpiece. As the result of this motion, the ground surface includes undesired integrity and, in some cases, damage. In addition, the increased grinding force associated with chatter vibration leads to accelerated wheel wear (Liao and Shiang, 1991). Workpiece burn during the grinding process is essentially a kind of an irreversible change in the microstructure of a surface layer. The burn occurs when workpiece is exposed to continuous high temperature at the grinding zone. A visual observation of a grinding burn is due to temper colors from very thin oxide layers on the workpiece surface. This layer of ferrous material is composed of Fe_2O_3, Fe_3O_4, and FeO membranes from the free surface. At the onset of a grinding burn, the grinding force and the rate of wheel wear increase sharply, and the surface roughness deteriorates. S. Malkin (1989) proposed a critical limit for grinding burn with respect to various items in surface grinding. According to his research, grinding burn appears easily on the surface of a workpiece when smaller abrasives, higher grades of grinding wheels and more hardened materials are used.

* Corresponding Author,
E-mail : jskwak@hyowon.pusan.ac.kr
TEL : +82-51-510-1419 ; **FAX** : +82-51-514-0685
Full Time Researcher, School of Mechanical Engineering, Pusan National University, San 30, Jangjeon-Dong, Kumjung-Ku, Pusan 609-735, Korea. (Manuscript **Received** February 18, 2000; **Revised** April 24, 2000)

Chatter vibration is a dynamic instability that occurs in most machining processes, including grinding, and is considered to be the most serious cause of deterioration of surface quality. In general, such vibration limits the productivity of machining operations and causes the deterioration of the integrity of workpiece surfaces. Moreover, during the grinding process, the growth of a wavy surface on the grinding wheel, a growth induced by chatter vibration, results in the need for the interruption of the grinding process to dress the wheel.

In this study, the neural network has been applied to grinding diagnosis system. The parameters of acoustic emission (AE) signals have been used as the inputs of the neural network.

2. AE Signal and Neural Network

2.1 Fault Phenomena and AE Signal

Grinding is often done in the final finishing of a component because of its ability to satisfy strict requirements of surface roughness. However, when a grinding fault generates, the allowable range of surface roughness cannot be maintained. Grinding burns often occur in workpieces, especially with adhesive materials. Metals adhering between voids within the grinding wheel constrict the action of machining. Therefore, the grinding operation becomes an abnormal state and the grinding temperature rapidly rises to about 1, 000℃. Due to the effects of the increased temperature, the surface of the workpiece is burnt. Chatter marks, which are normal to grinding direction, can appear on the ground surface. As the grinding burn or the chatter vibration occurs, the deterioration of the surface becomes evident.

In order to produce a product that solves grinding faults such as burn and chatter vibration, they must be monitored by credible methods.

The AE generated during a grinding process has been proven to contain information strongly related to the condition changes in the grinding zone (König et al., 1995; Wakuda et al., 1993; Dornfeld and Cai, 1984; Emel and Asibu, 1998). The investigation described in this paper uses AE signals to detect chatter vibration and grinding burn. The parameters for monitoring potential problems are the peak of RMS (Root Mean Square), the peak of FFT (Fast Fourier Transform), the count out of the threshold, and the standard deviation of acquired AE signals.

2.2 Back-propagation Algorithm

In the hope of achieving human-like performance, artificial neural networks have been studied for many years in the field of speech, image recognition and pattern classification (Bruck and Goodman, 1988; Widrow et al., 1975; White, 1989). Such neural networks are composed of many non-linear computational elements operating in parallel fashion. Neural networks, because of their massive nature, can perform computations at a higher rate. Because of their adaptive nature in using the learning process, neural networks can adapt to changes in the data and learn the characteristics of input signals. Learning in a neural network means finding an appropriate set of weights that are connection strengths from the elements of one layer to the elements of the next layer. In this study, the back propagation algorithm of neural networks, which is one of the learning modes, is used. The squared error (E_p) for the output layer and the weight-change equation are given by the following equations (Freeman and Skapura, 1991).

$$E_p=\frac{1}{2}\sum_k (T_{pk}-O_{pk})^2 \tag{1}$$

$$\frac{\partial E_p}{\partial W_{ji}}=\frac{1}{2}\sum_k \frac{\partial}{\partial W_{ji}}(T_{pk}-O_{pk})^2 = -\sum_k (T_{pk}-O_{pk}) f'_k(net_{pk})\, W_{kj} \times f'_j(net_{pj})\, X_{pi} \tag{2}$$

$$W_{kj}(t+1)=W_{kj}(t)+\alpha\ \delta_{pk} i_{pj} + m\Delta W_{kj}(t-1) \tag{3}$$

where W_{ji} is the weight on the connection from the ith input element to jth element of another layer, α is called the learning-rate parameter, and i_{pj} and δ_{pk} are presented as follows:

$$i_{pj}=\left(\frac{\partial}{\partial W_{kj}}\sum_{j=1}^{L} W_{kj}X_{pj}+\theta_k\right) \tag{4}$$

$$\delta_{pk}=T_{pk}-O_{pk} \tag{5}$$

m is the momentum coefficient, which increases in the speed of convergence for learning the

neural networks. X_{pi} is an input pattern, and f' ( ) indicates a derivative of sigmoid transfer function for each layer. T_{pk} is the teaching data, and O_{pk} is the output data of the neural networks.

3. Experiment and Results

3.1 Experimental Methods

Figure 1 shows a scheme of the experimental setup. A series of grinding tests were conducted on a cylindrical grinder with a 228 mm diameter, WA60LmV wheel, which is commonly used in workshops. An AE sensor with a frequency response of wide bands (100~800 kHz) was used to measure the signals generated during the grinding operation. The sensor was attached to the center of a grinding machine. To avoid signal attenuation during the transportation from the

Table 1 Conditions for obtaining AE signals

Items	Conditions
Grinding Wheel	Type: WA60LmV Size: $\phi 228 \times 24$ mm
Wheel Speed	V_s=27.1 m/s(1800 RPM)
Workpiece	Material: STD11 Hardness: H_RC 45
Workpiece Speed	V_w=0.15~0.30 m/s
Infeed Rate	0.5 mm/min(75 pieces) 1.0 mm/min(75 pieces) 2.0 mm/min(75 pieces)
Cutting Fluid	Dry Cut
Dressing	Single Pointed Diamond Dresser Depth of Cut: 0.0125 mm Lead: 0.015 mm/rev

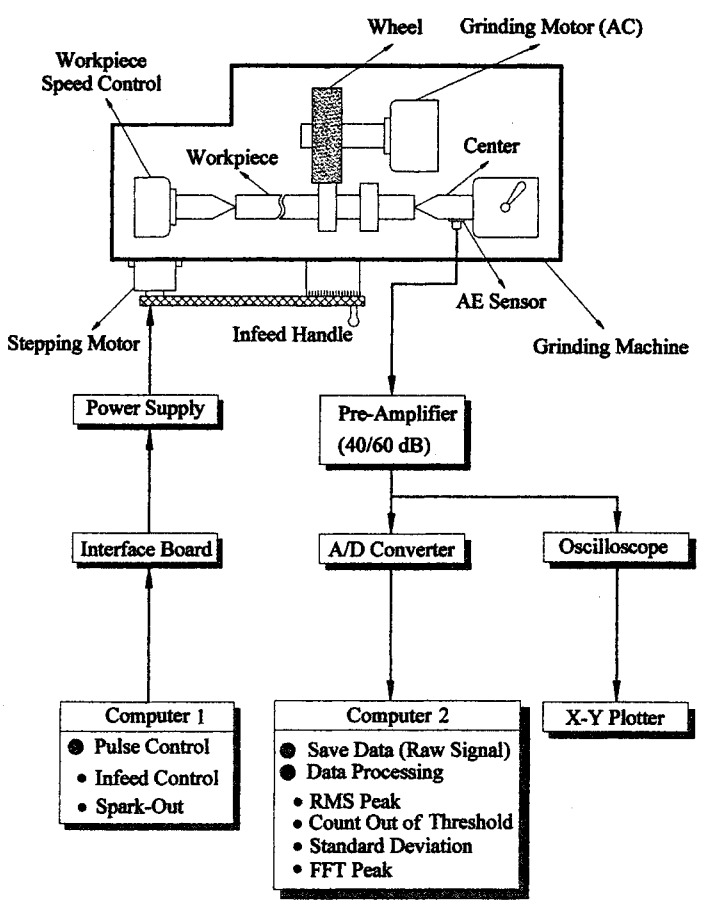

Fig. 1 Experimental setup for fault detection

sensor to a computer, a pre-amplifier was connected to the cable of signal flow and its auxiliary function was to filter the noise that disturbs the AE signals. The raw AE signals were digitized using an A/D converter Model PCL-818 and stored using a personal computer for later analysis. Stored signals were analyzed through data processing. Grinding conditions used in monitoring the AE signals are listed in Table 1.

3.2 Experimental Results and Discussions

Figure 2(a) shows typical AE signals obtained

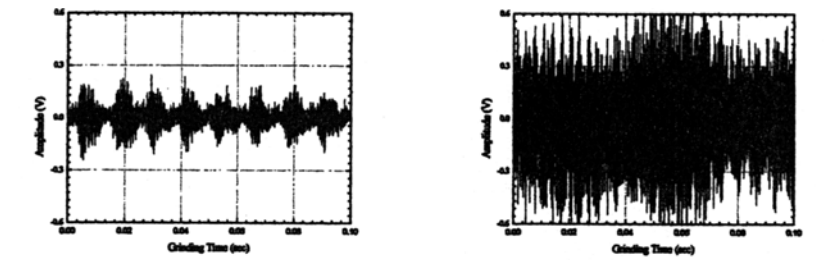

(a) Raw signals

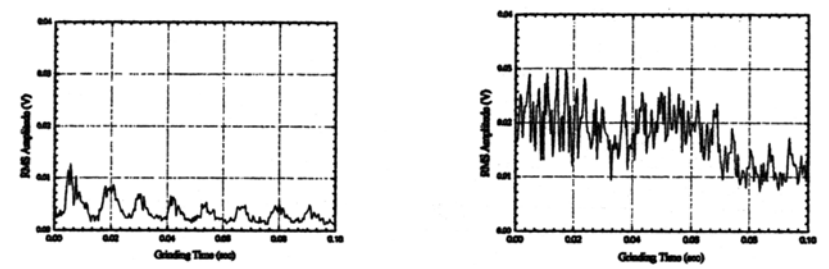

(b) RMS signals

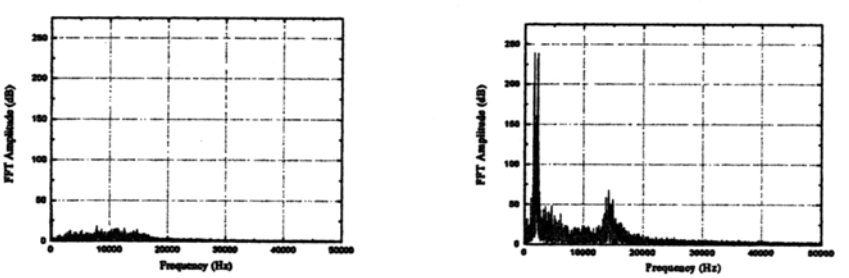

(c) FFT signals

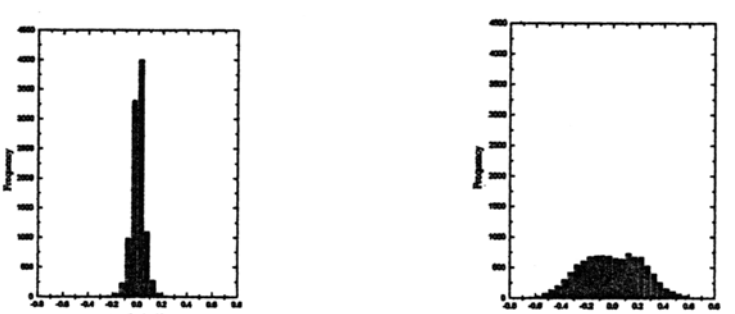

(d) Distribution

Fig. 2 Obtained AE signals and signal processing forms

from the grinding operation. As in other metal cutting processes, the raw signals are continuous types and sharply fluctuate with grinding time. The amplitudes of raw signals increase according to the number of ground workpieces, but because of the similitude in signals grinding states are not always distinguished either stable or unstable. Therefore, other analytic parameters are needed to identify the grinding state. Figure 2(b) presents the signal to process the RMS with the raw signal shown in Fig. 2(a). The changes in AE signals are easily verified by an AE RMS level and a distinctive type. The results of the frequency analysis with the raw signals are drawn in Fig. 2 (c). The FFT amplitude is evident, especially when the frequency ranges reach about 1.8 kHz and 15 kHz. Because the wheel rotational frequency is approximately 30 Hz, it can be seen that a fault frequency is an integer multiple of the wheel rotational frequency. When the sampled values have a sufficiently strong central tendency, then a standard deviation of the sampled values may be useful for characterizing the set. The standard deviation is the positive square root of the variance that reveals the degree of distribution for the sampled data. Figure 2(d) presents the distribution of AE signals, and it shows that the stronger central tendency is in a stable grinding state. Based on the above results, the parameters of the AE signals for monitoring faults have been selected, measured, and are shown in Figs. 3~6.

In Fig. 3, the peak values of RMS increase gradually according to the number of grinding pieces. It was found that the more the in-feed rates are applied, the higher the level of the RMS peak became. Figure 4 presents the peak values of FFT. The FFT's level maintains to a particular piece, as an example, the 25th piece with 2.0 mm/min in-feed rate, and after the 25th piece, the peak level increases suddenly. The boundary point of the change in peak values often implies the fault generated. In this case, chatter marks generated on the workpiece are experimently observed.

Figure 5 shows the count outs of the threshold over the 20 mV level of the acquired raw signal that was enumerated with a computer program. The threshold level is determined by a preliminary experiment. The increased count outs of the threshold may be considered as a sign of a fault.

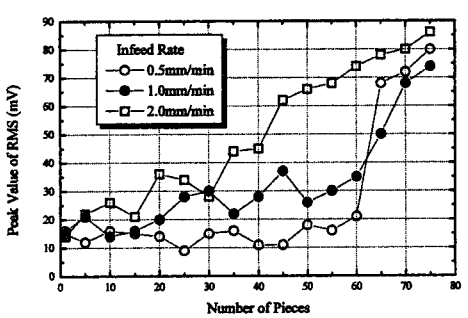

Fig. 3 RMS peak versus number of pieces

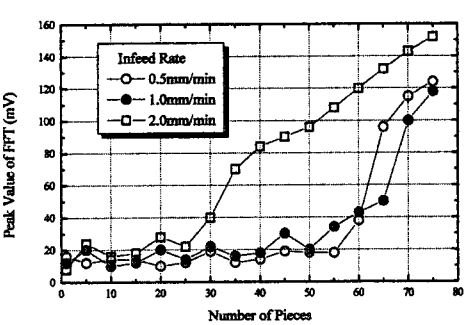

Fig. 4 FFT peak versus number of pieces

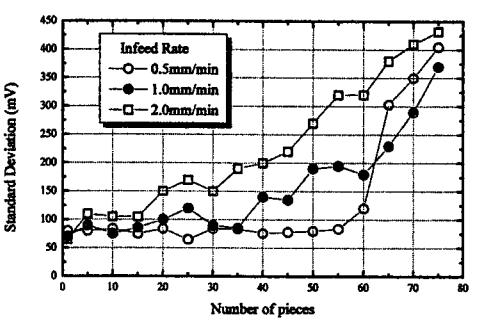

Fig. 5 Standard deviation versus number of pieces

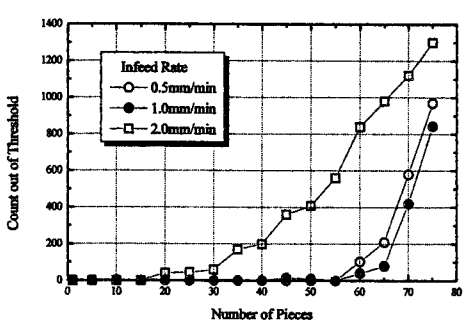

Fig. 6 Thershold count versus number of pieces

Figure 6 presents the standard deviation of the raw AE signals according to the number of grinding pieces. It can be seen that the value of the standard deviation increases when the number of ground pieces increases. By varying the parameters, a more effective diagnosis system for grinding fault can be established.

4. Fault Detection System

Depending on the selection of the above parameters, especially the learning-rate and the momentum coefficient, the performance of neural networks can vary widely. Therefore, it is necessary to optimize the neural networks with optimal parameters.

From the results shown in Fig. 7, which was obtained through a preliminary study, the value of the learning-rate and the momentum coefficient were found to be 0.6 and 0.8, respectively. Also, it was decided that the number of hidden layers would be two.

Simulations for implementing the system for diagnosing grinding faults were conducted on a personal computer. Figure 8 shows the architecture of the neural network used. The input units were the peak of the RMS, the peak of the FFT, the count out of the threshold, and the standard deviation of AE signals. Normal, burning, and chatter vibration states were used as the output parameters, which had the interval values from 0 to 1. In comparison with these values of output parameters, most major value of the parameters indicates the state of the grinding operation.

Table 2 presents the values of input parameters and the desired output based on the AE experimental results. At the desired output, each pattern has the value of unity (only one parameter) or zero. For example, the neural network has learned that the grinding pattern of AE-5 is

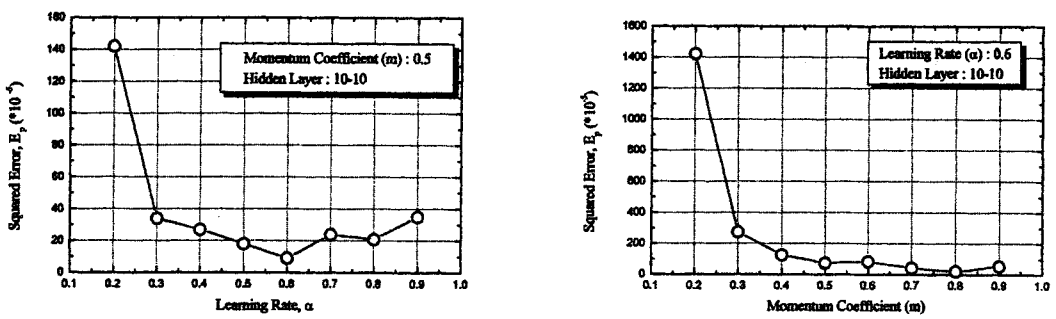

(a) Learning rate versus squared error (b) Momentum coefficient versus squared error

Fig. 7 Relationship between learning parameters and squared error

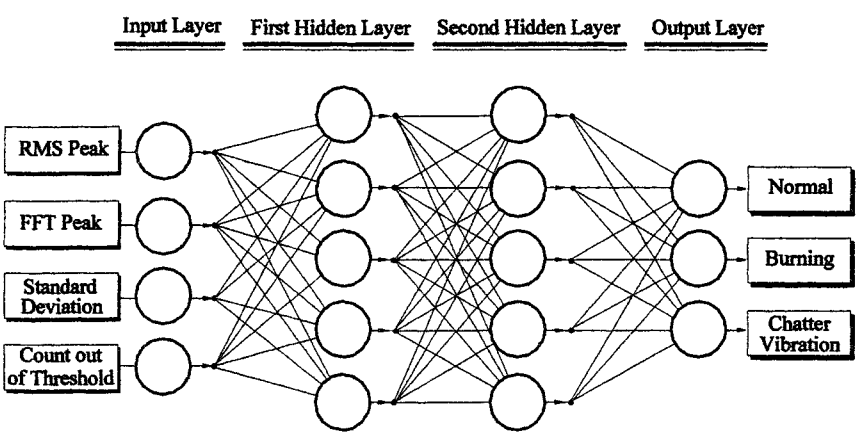

Fig. 8 Architecture of the neural network used in this study

Table 2 AE supervised data for the learning of neural network

Pattern	Input Parameters				Desired Output		
	RMS Peak	Standard Deviation	FFT Peak	Threshold Count	Normal	Burning	Chatter
AE-05	0.021	0.096	0.0200	0	1	0	0
AE-06	0.018	0.087	0.0081	0	1	0	0
AE-07	0.021	0.109	0.0138	0	1	0	0
AE-08	0.024	0.091	0.0093	0	1	0	0
AE-09	0.019	0.078	0.0069	0	1	0	0
AE-43	0.034	0.155	0.0245	10	0	1	0
AE-45	0.037	0.139	0.0409	23	0	1	0
AE-46	0.032	0.140	0.0223	9	0	1	0
AE-70	0.033	0.283	0.0490	48	0	0	1
AE-71	0.048	0.322	0.1130	626	0	0	1
AE-72	0.042	0.342	0.0664	931	0	0	1
AE-73	0.039	0.305	0.0569	607	0	0	1
AE-74	0.033	0.256	0.0382	68	0	0	1

Table 3 Recalled results of the AE data in neural network

Pattern	Input Parameters				Outputs of Neural Network			Results
	RMS Peak	Standard Deviation	FFT Peak	Count	Normal	Burning	Chatter	
AE-05	0.021	0.096	0.0200	0	0.987990	0.010019	0.010521	Normal
AE-06	0.018	0.087	0.0081	0	0.987986	0.010020	0.010523	Normal
AE-07	0.021	0.109	0.0138	0	0.987993	0.010019	0.010518	Normal
AE-08	0.024	0.091	0.0093	0	0.987988	0.010020	0.010522	Normal
AE-09	0.019	0.078	0.0069	0	0.987984	0.010020	0.010525	Normal
AE-43	0.034	0.155	0.0245	10	0.010223	0.813255	0.185224	Burning
AE-45	0.037	0.139	0.0409	23	0.010218	0.813217	0.185274	Burning
AE-46	0.032	0.140	0.0223	9	0.010221	0.813247	0.185241	Burning
AE-70	0.033	0.283	0.0490	48	0.010217	0.013243	0.985249	Chatter
AE-71	0.048	0.322	0.1130	626	0.010216	0.013242	0.985247	Chatter
AE-72	0.042	0.342	0.0664	931	0.010216	0.013242	0.985251	Chatter
AE-73	0.039	0.305	0.0569	607	0.010217	0.013242	0.985250	Chatter
AE-74	0.033	0.256	0.0382	68	0.010224	0.014232	0.985243	Chatter

normal, AE-43 indicates burning, and AE-70 indicates chatter vibration.

The recalled results that were obtained through the iterative learning of the established neural network are listed in Table 3. The outputs of the neural network coincide with the desired outputs shown in Table 2. This indicates that learning by the neural network has been successful and that this system for diagnosing grinding faults is able to recognize the various grinding states.

Table 4 Implementation results for new AE data

Pattern	Input Parameters				Outputs of Neural Network			Results
	RMS Peak	Standard Deviation	FFT Peak	Count	Normal	Burning	Chatter	
AE-10	0.014	0.075	0.0078	0	0.967983	0.010020	0.010525	Normal ○
AE-11	0.023	0.116	0.0165	0	0.957995	0.010018	0.010517	Normal ○
AE-12	0.023	0.111	0.0116	0	0.957993	0.010019	0.010518	Normal ○
AE-13	0.019	0.097	0.0144	0	0.967990	0.010019	0.010521	Normal ○
AE-14	0.019	0.105	0.0084	0	0.967992	0.010019	0.010519	Normal ○
AE-15	0.017	0.089	0.0108	0	0.947987	0.010020	0.010522	Normal ○
AE-44	0.034	0.194	0.0409	11	0.010223	0.613252	0.386741	Burning ○
AE-47	0.034	0.155	0.0372	13	0.010219	0.613252	0.386741	Burning ○
AE-48	0.033	0.158	0.0403	16	0.010217	0.613253	0.386746	Burning ○
AE-57	0.035	0.191	0.0314	20	0.010132	0.484631	0.542173	Chatter ×
AE-58	0.038	0.194	0.0410	24	0.010212	0.044217	0.563142	Chatter ×
AE-66	0.040	0.234	0.0450	156	0.010219	0.413252	0.586742	Chatter ○
AE-67	0.046	0.239	0.0493	258	0.010221	0.42355	0.606744	Chatter ○
AE-68	0.037	0.266	0.0451	114	0.010221	0.373253	0.616745	Chatter ○
AE-69	0.037	0.279	0.0387	94	0.010217	0.313255	0.676741	Chatter ○

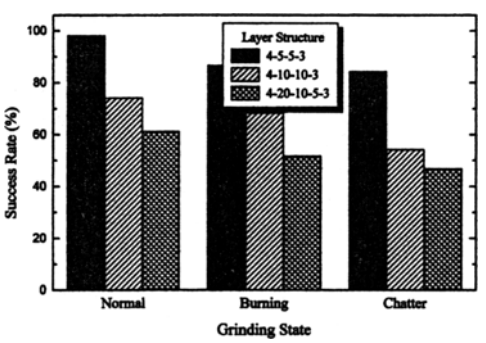

Fig. 9 Performance of the established fault diagnosis system

Table 4 lists the implementation results for new AE data, which were not learned in the previous step. In this case, the output values of the neural network have a few changes compared with the outputs listed in Tables 2 and 3. The normal parameters shown in Table 4 have a higher concentration of unity values when the normal state of the grinding operation is maintained. However, burning and chatter vibration parameters have a lower concentration of unity when burning or chatter vibration state is generated. Some erroneous recognition was made in the boundary points between burning and chatter vibration states.

Although lower concentration of unity and erroneous results occurred, the recognizable performance of the diagnosis system was very good. Figure 9 shows the respective percentages of the success rates according to the various layer structures in the diagnosis system. From Fig. 9, it is evident that the maximum performance becomes about 90% when the layer structure of the neural network is composed of 4-5-5-3 units.

5. Conclusion

A method using the AE signals has been developed for recognizing chatter vibration and grinding burn in the cylindrical plunge grinding process. The following conclusions can be drawn from the results of this study:

(1) When grinding faults such as chatter vibration and grinding burn occur, the values of the AE parameters for the peak of the RMS, the peak

of the FFT, the standard deviation, and the count out of the threshold all increase non-linearly. The more the in-feed rates are applied, the higher the levels of AE parameters become.

(2) The FFT amplitude is especially evident when the frequency ranges reach about 1.8 kHz and 15 kHz. Because the wheel rotational frequency is approximately 30 Hz, it is seen that a fault frequency is an integer that is a multiple of the wheel rotational frequency.

(3) Depending on the selection of parameters, especially the learning-rate and the momentum coefficient, the performance of neural networks can vary widely. To optimize a neural network for fault diagnosis, the value of the learning-rate and the momentum coefficient were respectively determined to be 0.6 and 0.8. Also, the number of hidden layers was determined to be two.

(4) Based on the implementation results of the computer simulation for new AE data that were not learned, it was found that the output values of normal parameters have a higher concentration of unity values when the normal state of the grinding operation is maintained. On the other hand, burning or chatter vibration parameters have lower concentrations of unity values when the burning or the chatter vibration occurs. Some erroneous recognition was made in the boundary point between burning and chatter vibration. The maximum performance became about 90% when the layer structure of the neural network is optimized.

References

Bruck, J. and Goodman, W., 1988, "A Generalized Convergence Theorem for Neural Networks," *IEEE Trans. Inform. Theory*, Vol. 34, pp. 1089~1029.

Dornfeld, D. and Cai, He Gao, 1984, "An Investigation of Grinding and Wheel Loading Using Acoustic Emission," *Transactions of the ASME*, Vol. 106, No. 2, pp. 28~33.

Emel, E. and Asibu, E. K., 1988, "Tool Failure Monitoring in Turning by Patterning Recognition Analysis of AE Signals," *Transactions of the ASME*, Vol. 110, No. 5, pp. 137~145.

Freeman, J. A. and Skapura, D. M., 1991, : *Neural Networks-Algorithms, Applications, and Programming Techniques*, Addison-Wesley Publishing Company, New York.

Kawamura, Suehisa and Mitsuhashi, Michio, 1981, "Studies on the Fundamental of Grinding Burn (3rd Report) Oxidation Rate Raw of Workpiece," *Journal of the Japanese Society of Precision Engineering*, Vol. 47, No. 9, pp. 106~111.

Kim, G. H., Inasaki, I. and Lee, J. K., 1994, "Architecture of Knowledge-Base and Management System for Grinding Operations," *Journal of the Korean Society of Precision Engineering*, Vol. 11, No. 1, pp. 211~218.

König, W., Altintas, Y. and Memis, F., 1995, "Direct Adaptive Control of Plunge Grinding Process Using Acoustic Emission Sensor," *The International Journal of Machine Tools and Manufacture*, Vol. 35, No. 10, pp. 1445~1457.

Liao, Y. S. and Shiang, L. C., 1991, "Computer Simulation of Self-Excited and Forced Vibtarions in the External Cylindrical Plunge Grinding Process," *Transactions of the ASME*, Vol. 113, No. 8, pp. 297~304.

Lindsay, P. and Hahn, S., 1971, "On the Basic Relationships between Grinding Parameters," *Annals of the CIRP*, Vol. 20, No. 5, pp. 657~671.

Malkin, S., 1989, *Grinding Technology-Theory and Applications of Machining with Abrasives*, John Wiley & Sons, New York.

Wakuda, M., Inasaki, I., Ogawa, K. and Takahara, M., 1993, "Monitroing of the Grinding Process with an AE Sensor Integrated CBN Wheel," *Journal of the Japanese Society of the Precision Engineering*, Vol. 59, No. 2, pp. 97~102.

White, H., 1989, "Learning in Artificial Neural Networks," *Neural Computation*, Vol. 1, pp. 425~464.

Widrow, B., et al., 1975, "Adaptive Noise Cancelling: Principles and Applications," *Proc. IEEE*, Vol. 63, pp. 1692~1716.